Ch 2. Global Climate—R. J. H. Dunn, D. M. Stanitski, N. Gobron, and K. M. Willett, Eds.

Author list

Barichivich, J., Instituto de Geografía, Pontificia Universidad Católica de Valparaíso, Valparaíso, Chile

Harris, I., National Centre for Atmospheric Science, University of East Anglia, Norwich, United Kingdom and Climatic Research Unit, School of Environmental Sciences, University of East Anglia, Norwich, United Kingdom

Jones, P. D., Climatic Research Unit, School of Environmental Sciences, University of East Anglia, Norwich, United Kingdom

Osborn, T. J., Climatic Research Unit, School of Environmental Sciences, University of East Anglia, Norwich, United Kingdom

van der Schrier, G., Royal Netherlands Meteorological Institute, De Bilt, The Netherlands

d. Hydrological cycle

11. Monitoring global drought using the self-calibrating Palmer Drought Severity Index—J. Barichivich, T. J. Osborn, I. Harris, G. van der Schrier, and P. D. Jones

Hydrological drought results from a period of abnormally low precipitation, sometimes exacerbated by additional evapotranspiration (ET), and its occurrence can be apparent in reduced river discharge, soil moisture, and/or groundwater storage, depending on the season and duration of the event. Here, an estimate of drought called the self-calibrating Palmer Drought Severity Index (scPDSI; Wells et al. 2004; van der Schrier et al. 2013) is presented, using precipitation and Penman-Monteith Potential ET from an early update of the CRU TS 4.04 dataset (Harris et al. 2014). Moisture categories are calibrated over the complete 1901–2019 period to ensure that "extreme" droughts and pluvials (wet periods) relate to events that do not occur more frequently than in approximately 2% of the months. This affects direct comparison with other hydrological cycle variables in Plate 2.1 that use a different baseline period.

Drought area according to the scPDSI decreased slightly across the globe in 2018 (Barichivich et al. 2019) and continued decreasing through early 2019, but then rose sharply after May (Fig. 2.d.11.1). The global land area undergoing extreme drought conditions increased from a minimum of 1.7% in May to 4.7% in December, surpassing the most recent previous peak of 4.3% in October 2017, but not as extensive as some earlier periods of extreme drought. Also from May to December 2019, the area including severe and extreme drought conditions increased from 7.2% to 12% of the global land area, while moderate or worse drought conditions increased from a minimum of 19.2% to 24.6% of the global land area.

Similar to 2018, moderate to severe drought conditions during 2019 were extensive in South America, the western United States, and the Middle East. Previous moderate to severe drought conditions over Europe, southern Africa, and Australia intensified to extreme drought (Plate 2.1s). The east–west moisture contrast observed across the United States since 2017 further strengthened in 2019, with extensive wetter conditions extending over the whole eastern half and drier in the west. Protracted drought over most of the semiarid northeastern region of Brazil (Jimenez-Muñoz et al. 2016) and central Chile (Garreaud et al. 2017) intensified again in 2019 (Fig. 2.d.11.2).

A large part of South Africa experienced extreme drought during 2019 (Plate 2.1s), continuing or intensifying (Fig. 2.d.11.2) dry conditions from previous years. In the Cape region, this is consistent with a long-term drying associated with human-caused climate change (Seager et al. 2019), which increases the risk of such rare events (Otto et al. 2018). Previous moderate to severe drought along parts of the west coast of Africa appear to have eased, while wetter conditions in most of central and eastern Africa persisted in 2019 (Fig. 2.d.11.2). However, these changes should be interpreted with caution since station data are sparse in these regions. See section 7e for more detailed precipitation analyses for Africa.

Extreme drought conditions that affected Afghanistan in 2018 eased through 2019, and the area under drought was reduced and concentrated mostly over the south of the country. Drought severity also decreased in parts of the Arabian Peninsula that have seen dry conditions since 2017 (Fig. 2.d.11.2). Most of Australia saw an increase in drought intensity to severe and extreme conditions due to the continuation of the rainfall deficit combined with record high temperatures. These extreme conditions contributed to the most devastating fire season on record. Fire spread through the southeastern states causing unprecedented devastation. Extreme drought in the Murray–Darling Basin has been characterized as the worst on record. See section 7h4 and Sidebar 7.6 for details.

Antecedent dry conditions, below-average spring precipitation, and extreme summer heatwaves pushed most of Europe into drought during 2019 (Plate 2.1s). The most intense drought to the annual average occurred across northern Germany and Poland, where there was already a strong soil moisture deficit in 2018 (Fig. 2.d.11.2). The sustained low precipitation in spring and summer in combination with exceptionally high temperatures in late winter-early spring—especially February—and the record-breaking temperatures in June and July further intensified the drought conditions in much of midlatitude Europe.

78 **References**

79 Barichivich J, Osborn TJ, Harris I, van der Schrier G and Jones PD (2019) Global climate:
80 Drought [in "State of the Climate in 2018"]. *Bulletin of the American Meteorological*
81 *Society*, 100, S39-S40.

82 Garreaud, R. D., Alvarez-Garreton, C., Barichivich, J., Boisier, J. P., Christie, D.,
83 Galleguillos, M., LeQuesne, C., McPhee, J., and Zambrano-Bigiarini, M.: The 2010–2015
84 megadrought in central Chile: impacts on regional hydroclimate and vegetation, Hydrol.
85 *Earth Syst. Sci.*, **21**, 6307-6327, https://doi.org/10.5194/hess-21-6307-2017, 2017.

86 Harris I, Jones PD, Osborn TJ and Lister DH (2014) Updated high-resolution grids of
87 monthly climatic observations - the CRU TS3.10 dataset. International Journal of
88 Climatology 34, 623-642 (doi: 10.1002/joc.3711).

89 Jimenez-Muñoz, J.C., C. Mattar, J. Barichivich et al. (2016) Record-breaking warming and
90 extreme drought in the Amazon rainforest during the course of El Niño 2015–2016.
91 *Scientific Reports*, 6:33130, DOI: 10.1038/srep33130.

92 Otto, F.E.L., Wolski, P., Lehner, F., Tebaldi, C., Jan van Oldenborgh, G., Higesteeger, S.,
93 Singh, R., Holden, P., Fučkar, N.S., Odoulami, R. and New, M. (2018) Anthropogenic
94 influence on the drivers of the Western Cape drought 2015 – 2017. Environmental
95 Research Letters, 13(12).

96 van der Schrier, G., Barichivich, J, Briffa, K.R. and Jones, P.D., 2013: A scPDSI-based
97 global dataset of dry and wet spells for 1901-2009. J. Geophys. Res. 118, 4025-4048,
98 doi:10.1002/jgrd.50355

99 Wells, N., Goddard, S. and Hayes, M. J., 2004: A Self-Calibrating Palmer Drought Severity
100 Index. J. Climate 17, 2335-2351.

101

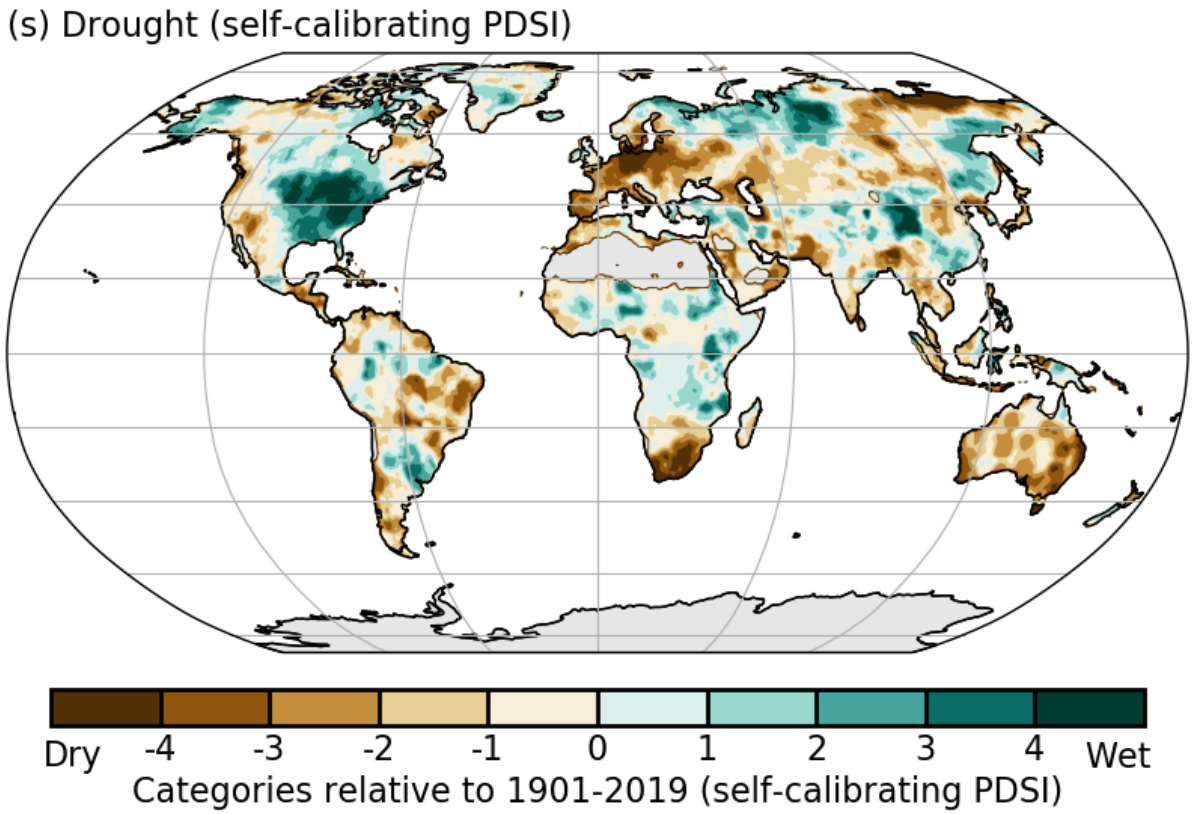

Plate 2.1s. Mean scPDSI for 2019. Droughts are indicated by negative values (brown), wet episodes by positive values (green). No calculation is made where a drought index is meaningless (gray areas: ice sheets or deserts with approximately zero mean precipitation).

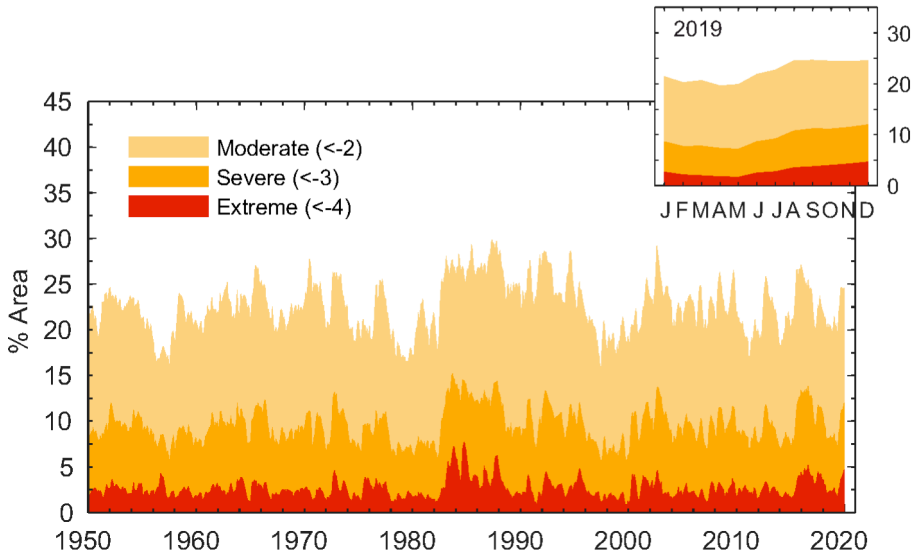

Fig. 2.d.11.1. Percentage of global land area (excluding ice sheets and deserts) with scPDSI indicating moderate (< −2), severe (< −3) and extreme (< −4) drought for each month of 1950–2019. Inset: Each month of 2019.

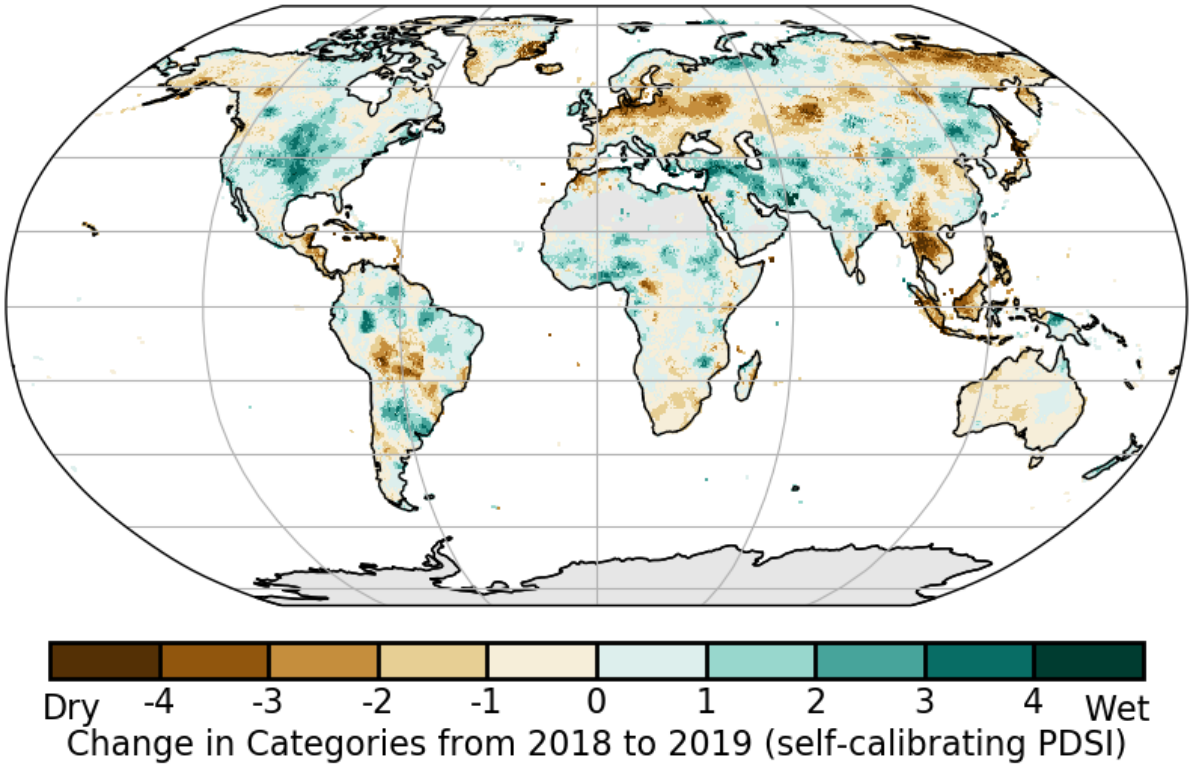

Fig. 2.d.11.2. Change in drought from 2018 to 2019 (mean scPDSI for 2019 minus mean scPDSI for 2018). Increases in drought severity are indicated by negative values (brown), decreases by positive values (green). No calculation is made where a drought index is meaningless (gray areas: ice sheets or deserts with approximately zero mean precipitation).